

Modulation of Impedance and Muscle Activation of the Upper Limb Joints while Simultaneously Controlling Manual-grasping and Walking

Joseph Mizrahi¹, Navit Roth¹ and Rahamim Seliktar²

¹*Department of Biomedical Engineering, Technion, Israel Institute of Technology, Haifa, Israel*

²*School of Biomedical Engineering, Science and Health Systems, Drexel University, Philadelphia, PA, U.S.A.*

Keywords: Mechanical Impedance, Muscle Activation, Motor Control, Manual-grasping, Balanced Walking, End-effector, Joint Constraints.

Abstract: The design of spring-based artificial and robotic arm joints presents a challenge in problems of transportation of manually-held objects during walking. For maintaining stability of these objects, stiffness and damping of the arm joints have to be adjusted by continuously tuning muscle activation. This necessitates knowledge about the mechanisms by which stiffness and damping (mechanical impedance) are being modulated in walking movement. The paradigm employed in this study consisted of modeling the impedance adjustments from input data obtained in simultaneously controlled grasping and walking experiments. While walking on a treadmill, tested subjects held a cup filled with liquid and were asked to aim at minimizing liquid spillage. Monitoring liquid spillage served to quantify stability of the hand as the end-effector of the upper limb. Kinematic data were obtained for the shoulder, elbow and wrist joints. Accelerometer data were obtained for the wrist and for the knee. Electro-myography (EMG) data were collected for the wrist flexor and extensor muscles. Based on the measured data, regressive functions were used to express stiffness and damping as a function of angle and angular velocity. The joints of the upper limb were thereafter successively constrained to study the effect of joint immobilization on joint impedance and muscle activation. The obtained results indicate the nonlinearity of the joint impedances as required in tasks of manual grasping of objects during locomotion, with and without joint constraints.

1 INTRODUCTION

Walking while grasping a cup filled with liquid (e.g. tea, water) is a common daily activity necessitating coordination of locomotion and prehension. Clearly, the aim in this task is to navigate the moving hand in space, so as to avoid or minimize spillage or dripping of liquid from the cup. Following unintended perturbations, it would also be desirable that the grasping hand regains its stability through motion of the joints of the upper limb. Thus, an interesting question is how our body controls these joint movements in order to perform the task in question.

Studying this question would provide an insight into the mechanisms, by which the stiffness and damping are adjusted to accommodate changes taking place during manual transport of objects while walking, if stability of the held object is to be maintained.

Mechanically, the upper limb can be represented by three major segments including the arm, forearm

and hand, connected through the shoulder, elbow and wrist joints. Through the motion of its joints, the upper limb provides the output to the terminal segment or end-effector: the self-navigating free hand grasping the cup of liquid being subjected to an oscillatory-like motion.

The complex relationship between torque, angular position and angular velocity, termed mechanical impedance, defines the stiffness and damping characteristics of the joint. Controlling the mechanical impedance of the upper limb joints is an important feature of the neuromuscular system enabling to stabilize hand-held objects in space, or to minimize the effect of externally applied forces (Stroeve, 1999).

Past studies on the combined control of the locomotor and prehensile systems have suggested that locomotion and reaching are closely connected motor activities (Georgopoulos and Grillner, 1989). More recently, mechanical aspects of the interaction between grasping and walking were reported (Roth et

al, 2011). Muscle activity was not included in this latter study.

The present study deals with the analysis of motion of the hand grasping a cup filled with liquid while walking. In order to explore the relative role of each of the joint to the mechanical impedances, different joint disabilities were simulated by the successive immobilization of each of the shoulder, elbow and wrist joints. Activation of the major muscle groups of the elbow joint was also studied by monitoring their EMG signals. Since impedance-based control strategies require information on the continuous nonlinear behavior of the joints, the results of the present research should have implications on the design of spring based artificial and robotic arms.

2 METHODS

Subjects ($n=4$), aged 28-57 (average 35.5, SD 14.3) provided informed consent to participate in the study according to the University's ethical committee's guidelines. The subjects walked on a treadmill (Woodway PPS55-Med) at a constant speed of 1.25 m/s while holding in their right hand a cup filled with liquid and fixing their look at a mark positioned in front of them at eye level. While walking, the subjects were instructed to maintain the liquid surface as level as possible, to minimize "liquid spillage" from the cup.

The walking tests, each of duration of 30 seconds, were performed in the following testing conditions: unrestricted joints of the upper limbs, followed by the successive restriction of each of the right wrist, elbow and shoulder joints. Joint restrictions were applied in order to immobilize each joint (wrist 180 degrees, elbow 90 degrees and shoulder 0 degrees). The restrictions were accomplished by means of constraining braces or straps. The tests were repeated five times at each condition with a resting period of 2 min between the tests.

3 INSTRUMENTATION

3.1 Apparatus for Liquid Spillage Quantitation

To observe the target of minimum liquid spillage, an instrumented cup was designed to monitor liquid level within the cup as follows, to simulate "liquid spillage". A plastic cup was wired at its inner surface

with circular conductive stripes, parallel to each other and to the bottom of the cup, to indicate different levels for the liquid. A signal was generated when the liquid (salted water) level raised as a result of the subject's motion and made contact with any of the circular stripes to short a circuit.

3.2 Kinematics

Since the joint angles served as inputs for the model, goniometers (Biometrics Ltd, Gwent, UK) were used for two-dimensional measurements of elbow and wrist angles. For kinematic measurements in the sagittal plane video data were collected by two-reflective markers located at the upper arm, near the shoulder and elbow joints, as shown in Fig. 1.

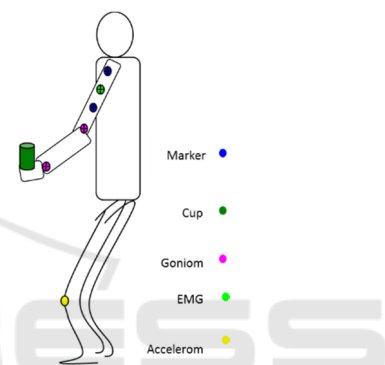


Figure 1: Positioning of sensors (blue=positioning marker, purple=goniometer, light green=EMG, yellow=accelerometer; the cup is shown in green color).

To monitor the foot-strike event, a light-weight accelerometer (Kistler PiezoBeam, type 8634B50) was attached onto the skin in closest position to the bony prominence of the tibial tuberosity and was aligned along the longitudinal axis of the tibia to provide the axial component of the vertical impact acceleration on the shank.

The signals from the accelerometer were fed to the PC-based data acquisition system at a sampling rate of 1000 Hz. A high sampling rate was required to pick-up the timings of the spike acceleration resulting from foot strike.

3.3 Electromyography (EMG)

Surface EMG signals from the right biceps and triceps muscles were monitored to indicate the activation of the major muscle groups of the elbow joint. The signals were measured by means of two pairs of bipolar Ag/AgCl disposable snap electrodes (10mm diameter), amplified (Atlas Research Ltd., Hod-Hasharon, Israel) and sampled at 1000 samples/s

(National Instrument AT-MIO-16E). The signals were processed as follows: in the time domain, the signals of each muscle were filtered (2-500 Hz), normalized to their respective maximal voluntary contraction (MVC) value, after which the root mean squares (RMS) were calculated. The co-contraction value of both muscles was calculated (Winter, 2009). In the frequency domain, steadiness of the median frequency was used to indicate the possible presence of muscle fatigue.

4 BIOMECHANICAL MODEL

The input to the system in Figure 1 are the periodic displacement signals due to the walking body-movement, as transmitted to the upper limb through the shoulder girdle, and the output of the system is the self-navigated free hand holding the cup-of-liquid. The model segments are assumed to be rigid bodies, with known mass and inertia properties. The joint angles are as defined in Fig. 2. The shoulder angle ϕ_s is defined between the upper arm and the vertical. Angles ϕ_e and ϕ_w represent the elbow and wrist joint angles, respectively, and their corresponding θ' are the external angles of these joints. Angles θ (no prime) are between segments and the horizontal. The model segments are connected together by the joints via lumped impedances representing damped springs.

The damped spring coefficients are expressible in terms of joint angles and angular velocities (Mizrahi, 2015).

Thus,

$$k_j(\phi) = k_{0j} + k_{1j}(\phi_j - \phi_{0j}) + k_{2j}(\dot{\phi}_j - \dot{\phi}_{0j}) \quad (1)$$

$k_j(\phi)$ – stiffness of joint j

$$b_j(\dot{\phi}) = b_{0j} + b_{1j}(\dot{\phi}_j - \dot{\phi}_{0j}) \quad (2)$$

$b_j(\dot{\phi})$ – damping of joint j

The reference angle ϕ_{0j} was taken in the neutral position of each joint.

These coefficients are related to joint torques M_j as follows:

$$k_j = \frac{\partial M_j}{\partial \phi_j} \quad (3)$$

$$b_j = \frac{\partial M_j}{\partial \dot{\phi}_j} \quad (4)$$

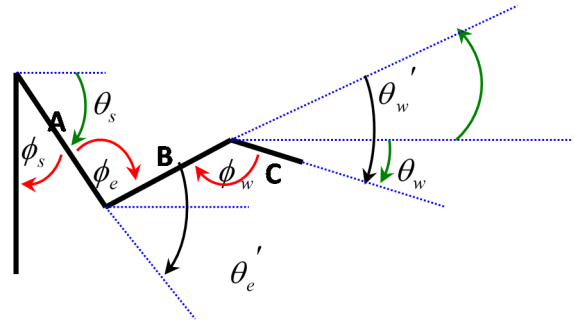


Figure 2: Sagittal view of segments and joints of the upper limb: A=upper arm, in relation of vertical axis of the body representing the walking body; B=forearm; C=hand.

The joint torque is M_j obtainable by integration and by summing up the elastic and damping torques.

$$\begin{aligned} M_{ij} = M_{stj} + M_{bj} = & \\ & k_{0j}(\phi_{ij} - \phi_{0j}) + \frac{k_{1j}}{2}(\phi_{ij} - \phi_{0j})^2 + \\ & k_{2j}[(\dot{\phi}_{ij} - \dot{\phi}_{0j})(\phi_{ij} - \phi_{0j})] + \\ & b_{0j}(\dot{\phi}_{ij} - \dot{\phi}_{0j}) + \frac{b_{1j}}{2}(\dot{\phi}_{ij} - \dot{\phi}_{0j})^2 \end{aligned} \quad (5)$$

The torques of the wrist, elbow and shoulder joints were obtained by solving the inverse dynamics for the upper limb using Kane's method (Kane and Levinson, 1985). These torques were thereafter used for the calculation of the stiffness and damping coefficients at each joint.

4.1 Parameter Estimation and Reduction of the Model

The stiffness and damping coefficients in Eqs. (5) were resolved from the calculated torques in the dynamic model by parameter estimation using optimization procedures. Parameter estimation was performed by using quadratic programming-LSQLIN. Comparison between the various testing conditions was carried out by using T-test for repeated measures and statistical significance was established at p-value $p < 0.05$. Parameter identification was made to reveal the joint impedance model which best fits all the tests made with and without joint restrictions, and to indicate whether the general impedance expressions could be reduced to a simpler form. To ensure correct parameter estimation, all predictor variables in the multiple linear regression analysis must be uncorrelated and the model

parameters should be independent of each other. Multiple collinearity diagnostic criteria combined with F-test (Rapoport et al 2003) were used to reveal dependencies and eliminate redundancies in the numerical solution of the stiffness and damping coefficients and reduce the variables in the stiffness and damping functions. The reduction procedure of the basic model was made separately for each joint.

5 RESULTS

In all four subjects, the liquid level did not reach the highest conductive stripe during steady-state motion. This indicated that the subjects succeeded in stabilizing their end-effector, irrespective of whether or not restrictions were introduced to the joints.

5.1 Joints Angles

Fig. 3 shows typical traces of the upper limb joint angles while walking and holding the cup-of-liquid. The traces shown are for the shoulder, elbow and wrist angles. The dark dots designate heel-strike events of the right foot.

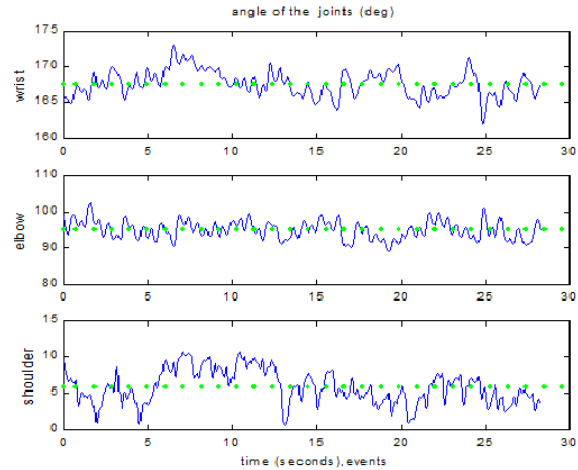


Figure 3: Typical traces of shoulder, elbow and wrist angles during test. The dark dots designate heel-strike events of the right foot.

Table 1: Overall stiffness (for the wrist, elbow and shoulder, expressed in N*m/rad) with and without joint restrictions. The values presented are averages of 5 tests, each over the period of 30 s (SD).

Restriction	Subject	Shoulder	Elbow	Wrist
No	1	46.63 (12.83)	3.02 (0.05)	3.53 (0.01)
	2	18.33 (0.45)	1.66 (0.36)	1.74 (0.01)
	3	42.02 (8.39)	2.05 (0.24)	2.141(0.03)
	4	21.02 (1.16)	2.10 (0.14)	8.97 (0.00)
Wrist	1	57.36 (8.42)	2.90 (0.49)	22.26 (0.06)
	2	36.28 (3.99)	1.73 (0.14)	1.42 (0.02)
	3	54.74 (6.56)	1.99 (0.08)	16.86 (0.27)
	4	19.58 (1.57)	1.99 (0.16)	126.65 (0.35)
Elbow	1	39.39 (4.14)	4.28 (0.43)	2.50 (0.01)
	2	47.61 (2.44)	3.39 (0.26)	1.90 (0.04)
	3	53.84 (5.73)	2.51 (0.24)	1.42 (0.00)
	4	19.70 (1.39)	3.03 (0.06)	4.14 (0.01)
Shoulder	1	64.91 (1.07)	3.60 (0.11)	2.67 (0.00)
	2	26.52 (1.89)	1.95 (0.49)	5.82 (0.19)
	3	52.77 (3.42)	1.72 (0.28)	2.18 (0.04)
	4	59.92 (8.74)	2.67 (0.08)	6.58 (0.02)

5.2 Model Reduction

By applying the multiple collinearity diagnostic criteria, the most significant stiffness coefficients (with p-value $p < 0.05$) were k_0 and k_2 , for the elbow and shoulder joints and k_0 for the wrist joint (Eq 1). The damping coefficient b_0 (Eq 2) was significant only in the wrist joint. Thus, it was concluded that reducing the optimal model to a 3-parameter model, with nonlinearly variable stiffness and constant damping would be sufficient, as follows:

For the wrist joint:

$$k_j(\phi) = k_{0j} \quad (6)$$

$$b_j(\dot{\phi}) = b_{0j} \quad (7)$$

For the elbow and shoulder joints:

$$k_j(\phi) = k_{0j} + k_{2j}(\dot{\phi}_j - \dot{\phi}_{0j}) \quad (8)$$

Table 1 presents values of the overall stiffness (Eqs. 6,8), in N*m/rad, with and without joint restriction. The values designate averages of 5 tests, each over the period of 30 s. The 'no restriction' case served as a reference for comparisons (t-test), with significance p level of $p < 0.05$.

During the tests with no restriction, the overall stiffness values were higher in the shoulder joint than

in the elbow and wrist joints. Wrist restriction resulted in an increase in stiffness (and damping) in that joint in 3 out of the 4 subjects. The effect on the elbow stiffness was a decrease in 3 out of 4 subjects. The effect on the shoulder stiffness was an increase in 3 out of 4 subjects. Elbow restriction demonstrated a stiffness increase in that joint. The effect on the wrist was a decrease in stiffness in 3 out of the 4 subjects (the effect on damping was not uniform). Elbow restriction did not cause any uniform effect on

the stiffness of the shoulder. Shoulder restriction resulted in an increase in stiffness on that joint. In 2 subjects this restriction resulted in a decrease in stiffness in the wrist and in 3 subjects an increase in stiffness in the elbow.

5.3 EMG Results

EMG traces (linear envelope of filtered data) of the biceps muscle alongside the elbow joint angle variation and elbow stiffness during a typical test without joint constraint are demonstrated in Fig. 4. The heel-strike signals are also shown by the red dots. It is seen that biceps EMG and elbow overall stiffness are opposite in phase. No correlation, however, was observed between EMG and joint angle. It should be remembered that stiffness is estimated from the model and is not directly expressed by the angle.

Summary of time-domain processing of the root mean square (RMS) values of the EMG signals is presented in Table 2 for one of the tested subjects. It is noted that activation intensity of the triceps is nearly 50% of that of the biceps. The results indicate that activation of both the biceps and the triceps were not significantly affected by constraining any of the wrist, elbow or shoulder joints. Likewise was the case for co-contraction of these two muscles. Median frequency results did not indicate development of fatiguing during the course of the tests.

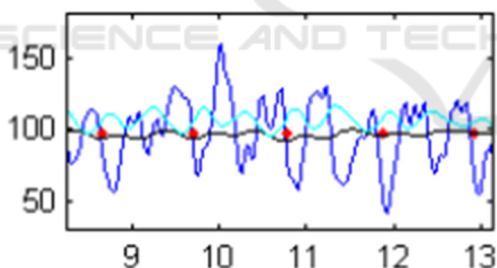


Figure 4: Filtered EMG signal of biceps (linear envelope) with no joint restriction (Blue line = EMG, light blue = elbow joint stiffness, black line = elbow joint angle, red dots = heel-strike events of right foot).

Table 2: Representative RMS values of the EMG results (normalized to MVC) of Biceps and Triceps muscles and of co-contraction. Both unconstrained and joint-constrained cases are reported.

Joint constraint	Biceps RMS	Triceps RMS	Co-contraction
No	3.284 (0.0130)	1.659 (0.0090)	68.20 (0.080)
Wrist	3.284 (0.0086)	1.664 (0.0037)	68.25 (0.080)
Elbow	3.274 (0.0082)	1.655 (0.0041)	68.15 (0.045)
Shoulder	3.266 (0.0078)	1.653 (0.0057)	68.21 (0.093)

6 DISCUSSION

Although coordination between locomotion and control has been studied in the past (Georgopoulos and Grillner, 1989; van der Wel and Rosenbaum 2007, Roth et al 2011), no works were found dealing with adjustment of the mechanical impedance by continuously tuning muscle activation during simultaneous control of grasping and walking.

The basic muscle-tendon model used was made to include elastic and damping elements. The elastic element depended on angular displacement and angular velocity (Woo and Young, 1991) and the damping element depended on angular velocity (Milner and Cloutier, 1998). By checking for multi co-linearity, this model was separately reduced and adapted to each of the joints, in accordance with the goodness of fit of parameter estimation.

The wrist joint was found to have constant stiffness and damping (Eqs 6,7), and no regulation of these coefficients was necessary during the gait cycle. It should be reminded, however, that the finger joints were not represented in the end-effector and this segment was considered a rigid body attached to the wrist joint. This representation was consistent with the two-dimensional assumption of the model. The other two joints had non-linear stiffness representations (Eq 7). Non-linear models are widespread in the description of human joints (Rakheja et al 1993; Karniel and Inbar, 1999; Konczack et al, 1999; Rapoport et al 2003). Both in the elbow and shoulder joints, stiffness included a constant coefficient as well as an angular velocity-dependent coefficient.

The EMG results did not confirm a definite relation between any of the elbow stiffness or elbow joint angle and the activation of the flexor and extensor muscles studied. It should be mentioned that intensity of these muscles relative to their respective MVC was only around 5% for the triceps and 10% for the biceps muscles. This low activation suggests that, most probably, other muscles (not monitored in this study) also take part in controlling the elbow joint, hindering the correlation sought. From the data of stride timing versus biceps EMG it can be noted that activation of this muscle decreases upon heel-strike and increases again towards the next strike. In view of the obvious presence of additional muscles in the process of elbow control, this particular behavior of the biceps should not be considered representative of the other muscles. Siegler et al (1985) also reported that joint torque and muscle activation are not uniquely correlated.

We did not find in this study a pre-activation of the muscles studied, prior to the impact loading

introduced by heel strike. Previous studies have indicated the presence of pre-activation in non-repetitive activities such as ball-catching (Lacquaniti et al, 1993). In the present study, loading was rather repetitive, due to the cyclic nature of steady walking.

7 CONCLUSIONS

We investigated how the stiffness and damping of the upper limb joints are being modulated in combined activity of hand grasping and locomotion. Kinematic data from the upper limb and of EMG from the wrist extensors and flexors were obtained with the joints unconstrained and after successively immobilizing each of the joints. Stiffness and damping values of each of the joints were obtained as a function of joint angle, for the shoulder and elbow joints. The wrist joint was found to have constant stiffness and damping, and no regulation of these coefficients was necessary during the gait cycle. The results also showed how joint immobilization affects the joint impedance behavior. The EMG results did not confirm a definite relation between any of the elbow stiffness or elbow joint angle and the activation of the flexor and extensor muscles studied. The wide variability in the impedance results obtained indicated that the compensatory mechanisms exercised by each subject to regulate the mechanical impedance to overcome the joint restriction were individual, not necessarily indicating to a common pattern. This study sheds light on the mechanisms of stabilization of grasped objects during walking and the results obtained, despite their variability, may be relevant for the future designing of artificial arms and robots and for the development of more accurate control strategies of combined hand grasping and walking.

REFERENCES

- Georgopoulos AP, Grillner S (1989) Visuomotor coordination in reaching and locomotion. *Science* 245:1209-1210
- Kane TR, Levinson DA (1985) *Dynamics: Theory and Application*. McGraw-Hill Book Company, New York
- Karniel A, Inbar GF (1999) The use of nonlinear muscle model in explaining the relationship between duration, amplitude, and peak velocity of human rapid movements. *J Motor Behav*, 31(3):203-206
- Konczak J, Brommann K, Kalveram KT (1999) Identification of time varying stiffness, damping and equilibrium position in human forearm movements. *Motor control* 3:394-413
- Lacquaniti F, Carrozzo M, Borghese NA (1993) Time varying mechanical behavior of multijointed arm in man. *J Neurophysiol* 69(5):1443-1464
- Milner TE (2002) Contribution of geometry and joint stiffness to mechanical stability of the human arm. *Exp Brain Res* 143:515-519
- Mizrahi, J. (2015) DOI: 10.1007/s40846-015-0014-y Mechanical Impedance and Its Relations to Motor Control, Limb Dynamics, and Motion Biomechanics, *J. Med. Biol. Eng.*, 35 (1):1-20, DOI 10.1007/s40846-015-0016-9.
- Rakheja S, Gurram R, Gouw GJ (1993) Development of linear and nonlinear hand-arm vibration models using optimization and linearization techniques. *J Biomech* 26(10):1253-1260
- Rapoport S, Mizrahi J, Kimmel E, Verbitsky O, Isakov E (2003) Constant and variable stiffness and damping of the leg joints in human hopping. *J Biomech Eng* 125:507-514
- Roth, N., Seliktar, R. and Mizrahi, J. (2011) Mechanical Impedance Control in the Human Arm while Manually Transporting an Open-Top Fluid Filled Dish, *Appl. Bionics and Biomechanics*, 8:393-404.
- Siegler S, Hillstrom HJ, Freedman W, Moskowitz G (1985) Effect of myoelectric signal processing on the relationship between muscle force and processed EMG. *American J of Physical Medicine* 64(4):130-149
- Stroeve S (1999) Impedance characteristics of neuromusculoskeletal model of the human arm. I. posture control. *Biol Cybern* 81:475-494
- Van der Wel RPRD, Rosenbaum DA (2007) Coordination of locomotion and prehension. *Exp Brain Res* 176:281-287
- Winter DA. *Biomechanics and motor control of human movement*. John Wiley and Sons, Inc., Hoboken, NJ; 2009.
- Woo SLY, Young EP (1991) Structure and function of tendons and ligaments. In: Mow VC and Hayes WC (eds) *Basic Orthopedic Biomechanics*, 2th edition. Raven Press, New York, pp199-243
- Zajac F E, Winters JM (1990) Modelling muscle system-joint and body segmental Dynamics' musculoskeletal actuation, and neuromuscular control. In: Winters JM and Woo SL-Y (eds) *Multiple Muscle Systems: Biomechanics and Movement Organization*. Springer-Verlag, New York, pp121-148